Electro-mechanical properties of poly(vinylidene fluoride-hexafluoropropylene) reinforced with zinc oxide nanostructure

Kittirat Phooplub[1,2], *Nantakan Muensit*[1,2] ✉

[1]*Department of Physics, Faculty of Science, Prince of Songkla University, Songkhla 90110, Thailand*
[2]*Center of Excellence in Nanotechnology for Energy (CENE), Prince of Songkla University (PSU), Hat Yai 90112, Thailand*
✉ *E-mail: nantakan.m@psu.ac.th*

Published in Micro & Nano Letters; Received on 20th February 2018; Revised on 31st March 2018; Accepted on 9th April 2018

The piezoelectric poly(vinylidene fluoride-hexafluoropropylene) ((P(VDF-HFP)) has been incorporated with zinc oxide (ZnO) of different forms, i.e. nanoparticles (NPs), nanorods (NRs), and microrods (MRs). The polymer has been activated the piezoelectric phase with the poling filed of 70 MV/m at 90°C for 10 min. ZnO of various particle types is grown into piezoelectric wurtzite. The addition of ZnO has slightly changed the degree of crystallinity of the polymers and clearly increased the elasticity to the best value in the case of inserted MRs. The electroactive phase of the polymer-based film has been enhanced at 2 wt% of ZnO for both NPs and NRs cases. The dielectric constant of the films increased with ZnO concentration. Finally, a cantilever beam structure with the patch of P(VDF-HFP) reinforced with ZnO of 2 wt% NRs shows the best performance as a microsource of the energy of about 1 μW. Development of micropower energy harvesting in P(VDF-HFP) with ZnO NRs has been substantially and highly promising to power small-scale electronics.

1. Introduction: A ceramic mixed in a host polymer has been manufactured to achieve good flexibility and high electroactivity for years [1–3]. The coupling between mechanical and electrical properties, i.e. piezoelectric effect existed in the active phases of ceramic and a polymer matrix has been gained much attention for various applications such as transducers, actuators and so on [4–6]. Recent progress in low-power, wireless microelectronic devices have raised an increased interest in harvesting energy using piezoelectric polymers due to view points of material engineering and economic conditions [7]. Amongst piezoelectric polymers, poly(vinylidene fluoride) (P(VDF)) has been widely studied, including its two copolymers, i.e. P(VDF)-hexafluoropropylene (P(VDF-HFP)) and PVDF-trifluorethylene. So far, there have been only a few reports on piezoelectric P(VDF-HFP) which is relatively good mechanically response to an electrical stimulus and much cheaper than P(VDF) [8]. Various fillers such as graphene, carbon black, and lead zirconate titanate including zinc oxide (ZnO) have been used to reinforce a polymer. This work focuses on ZnO which is often available in a field of anti-bacterial agent [9, 10] but not as a piezoelectric filler. There have also previous reports on ZnO nanowire in energy harvesting applications [11–13] but a few types of research are reported about its implementation on the electro-mechanical properties of a P(VDF-HFP) composite [14]. In this work, piezoelectric ZnO of different particle types which are nanoparticles (NPs), nanorods (NRs), and microrods (MRs) have been comparatively investigated their effect on the piezoelectric P(VDF-HFP). This is to extend the materials into an application as a microsource of energy which is an important issue for our future outlook. Since both materials are piezoelectric, and polymers generally suffer from relatively low piezoelectric coefficients. Developing a guideline to this problem is of useful for scientific and engineering viewpoint.

2. Materials and methods

2.1. Preparation of ZnO nanostructures: ZnO NPs and NRs were synthesised according to Harnack *et al.* [15]. The powder of zinc acetate dihydrate ($Zn(CH_3COO)_2{\cdot}2H_2O$, ≥98%, Sigma-Aldrich) of 29.5 g was dissolved in 125 ml methyl alcohol (J.T. Beaker) and 14.8 g of potassium hydroxide (KOH, 85%, Merck) was separately dissolved in 65 ml methyl alcohol (CH_3OH, 99%, J.T. Baker). The solutions were mixed at 60°C. NPs were obtained after 3 h while it took three days to obtain NRs. The solutions were rinsed several times with methyl alcohol. MRs were prepared by adapting the method of Greene *et al.* [16]. A seeding solution was prepared by mixing of 0.01 M $Zn(CH_3COO)_2{\cdot}2H_2O$ and 0.03 M sodium hydroxide (NaOH, 98%, Sigma-Aldrich) in methyl alcohol. The mixture was stirred at 60°C for 2 h. The seeding solution of 1 ml was then injected into the mixture of 25 mM zinc nitrate hydrate ($Zn(NO_3)_2{\cdot}xH_2O$, 99.999%, Sigma-Aldrich) and 25 mM hexamethylene tetramine (HMTA, 99%, Sigma-Aldrich) in deionised water at 90°C. The solution was stirred for 3 h. Afterwards, the solution was cooled down to room temperature, the precipitated ZnO was filtered and calcined at 600°C to obtain ZnO MRs.

2.2. Preparation of P(VDF-HFP) thin films: P(VDF-HFP) powder (Solef 11010/1001, 90:10 wt%, Solvay Solexis) dissolved in N,N-dimethylformamide (DMF, 99%, Sigma-Aldrich) with a weight fraction of 250 mg/ml was prepared. The solution was stirred at 40°C for 2 h. After that, the solution was kept at room temperature (18°C) until all air bubbles disappeared. The solution was casted on a glass substrate by using an adjustable film applicator (H.J. Unkel Limited) and dried at 90°C for 2 h. To exhibit the piezoelectricity, the films were undergone the constant electric fields of about 70 MV/m at 90°C for 10 min [8]. To assemble the piezoelectric films an indium tin oxide coated polyethylene terephthalate (ITO-PET, 60 Ω/square, Sigma-Aldrich) was used as a top electrode and a copper tape with carbon ink was underneath. The samples were then enamelled by a thermoplastic film at 130°C.

2.3. Characterisation of ZnO formation and AFM measurement: All the synthesised ZnO were imaged by using either transmission electron microscope (TEM, JEM-2010, JEOL Ltd.) or scanning electron microscope (SEM, FEI Quanta 400). The distribution of NPs in P(VDF-HFP) matrix was visualised by using a backscattering mode of the SEM. X-ray diffraction pattern and crystallinity of the polymer films were evaluated by using X-ray diffractometer (X'Pert MPD, Philips, the Netherlands).

Functional groups of the polymer were studied via a Fourier transform infrared spectrometer (FT-IR, LUMOS 70, Bruker).

P(VDF-HFP) has molecular formula as $(–CH_2CF_2–)_x[–CF_2CF(CF_3)–]_y$. The electroactive fraction is able to evaluate from an absorption at 840 cm^{-1} which is assigned to a mixed mode of CH_2 rocking and CF_2 asymmetric stretching vibration of electroactive β-phase, and in-plane bending of as-received α-phase at 776 cm^{-1} [17]. By using (1), the fraction can be calculated from the following equation:

$$F_{EA} = \frac{A_\beta}{\left((K_\beta/K_\alpha)\right)A_\alpha + A_\beta} \tag{1}$$

where K_α and K_β are the absorption coefficients at the respective wavenumber whose the values are 6.1×10^4 and 7.7×10^4 cm^2 mol^{-1} [18], respectively.

Elastic modulus was evaluated by using nanoindentation technique through an Atomic Force Microscope (AFM, Nanosurf Easyscan2, Nanosurf) and fitting the obtained force–distance curve to Hertz's theory [19]. A contact between the cantilever tip and a sample was mannered as a half sphere placed on a flat surface. A relationship between contact area and elastic modulus is given by

$$a_{\text{Hertz}} = \left(\frac{RF}{K}\right)^{1/3} \tag{2}$$

where R is the tip radius, F is the applied force through the cantilever tip, a_{Hertz} is the contact radius related to Z scanner and deflection of the cantilever by $a_{\text{Hertx}} = \sqrt{R(Z-\delta)}$ and K is the reduced elastic modulus given by

$$\frac{1}{K} = \frac{3}{4}\left(\frac{1-\upsilon^2}{E} + \frac{1-\upsilon_t^2}{E_t}\right) \tag{3}$$

where E and υ are elastic modulus and Poisson's ratio, respectively. The sharp tip apex (<10 nm) is for approaching a polymer. Before using to observe the deformation of the cantilever, the laser sensor of the AFM has been calibrated by approaching the cantilever to a glass surface [20]. The system sensitivity is 7.82×10^{-7} m/V.

2.4. Characterisation of the electro-mechanical properties: A dielectric constant for all the polymer-based films was measured by using LCR Meter (IM 3533, HIOKI) with dielectric test fixture probe (16451B, Agilent). The ability for energy harvesting of the film was tested by using the setup shown in Fig. 1.

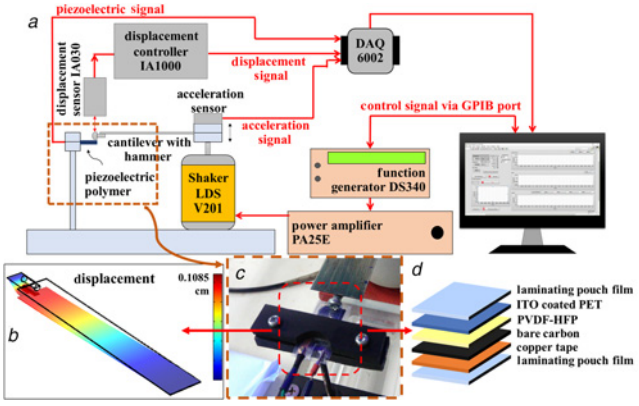

Fig. 1 *Energy harvesting setup*
a Schematic view of the setup for piezoelectric energy harvesting
b Chosen configuration consists of a cantilever beam as a hammer and piezoelectric harvester at the free end of the beam
c Photograph of the beam configuration
d Physical structure of piezoelectric harvester

An energy harvester of cantilever beam structure is chosen in this work due to its simplicity to implement at a low operating frequency (<100 Hz). The beam was fixed at one end and another was free. The equation of motion for transverse vibration and eigenfrequency to describe the mechanism of a uniform cross-sectional cantilever beam of length l is derived from the Euler–Bernoulli theorem as given by

$$w(x, t) = \Phi(t)X(x) \tag{4}$$

$$\Phi(t) = D_1 \sin \omega t + D_2 \cos \omega t \tag{5}$$

$$X(x) = C_1\left(\sin \alpha x + \frac{C_2}{C_1}\cos \alpha x + \frac{C_3}{C_1}\sinh \alpha x + \frac{C_4}{C_1}\cos \alpha x\right) \tag{6}$$

$$(\alpha l)^2 = \omega l^2 \sqrt{\frac{\rho A}{EI}} \tag{7}$$

where w is the deformation of the beam. The constants C and D can be obtained by the application of boundary conditions and normalisation. Equation (7) is a corresponding non-dimensional frequency for a solution depending mainly on the dimension of the beam. A location to patch a piezoelectric polymer onto the beam maximising energy conversion was done by using a finite element analysis (FEA) through the COMSol Multiphysics software (COMSOL 4.2 Update 3, USA). P(VDF) and its material property [21] was used as a piezoelectric device in the simulation. In the model, the piezoelectric film was sandwiched by a plastic film of the density of 1380 kg/m^3 and an elastic modulus of 2 GPa. A configuration that generated a higher mechanical strain of the polymer was chosen.

A cantilever ($135.0 \times 2.0 \times 0.5$ mm^3) made of spring steel with a hammer at the end was mounted on a permanent magnet shaker (V201, LDS Test, and Measurement) that was controlled via function generator (DS340, Stanford Research System). A vibration of the cantilever was detected by a CMOS laser analogue sensor with a controller (IA030, IA1000, KEYENCE). The cantilever was vibrated at 32 Hz with 15 g m/s^2 acceleration along the experiment. The generated signals from piezoelectric polymer were recorded by USB data acquisition module (DAQ6002, Nation instrument). All instruments were controlled via LabVIEW software package (LabVIEW 2013, Nation instrument).

3. Results and discussion

3.1. ZnO formation in the P(VDF-HFP) matrix: The SEM images of different forms of synthesised ZnO were shown in Fig. 2. The NPs in Fig. 2*a* have an average diameter of 6.25 ± 1.20 µm with an aspect ratio of 1. Some of the NPs have fused along their identical crystal faces and formed the oriented chains into the NRs. Subsequently formed NRs in Fig. 2*b* are 11.20 ± 2.63 nm in diameter and 62.99 ± 18.53 µm in length with an aspect ratio of 5.62. The MRs in Fig. 1*c*, respectively, have average length and diameter of 606 ± 166 nm and 71 ± 16 nm with an aspect ratio of 8.53. Most MRs dispersed randomly in the matrix. In case of NPs and NRS, the bright spots of the visualised mode are bigger than the particle size caused by the agglomerated particles.

3.2. Properties of the P(VDF-HFP) film with and without ZnO: XRD patterns of ZnO doped P(VDF-HFP) were shown in Fig. 3. The semi-crystalline structure with α-phase of the bare P(VDF-HFP) was confirmed by the diffraction peaks at $2\theta = 18.2°$, 20.0°, 26.6°, and 38.0°, corresponding to the (100), (020), (110), and (021) crystalline planes [14], respectively. With ZnO dopants, their diffraction peaks appeared at 31.82, 34.54, and 36.42, corresponding to the (100), (002), and (101) of wurtzite ZnO [22].

doi: 10.1049/mnl.2018.0148

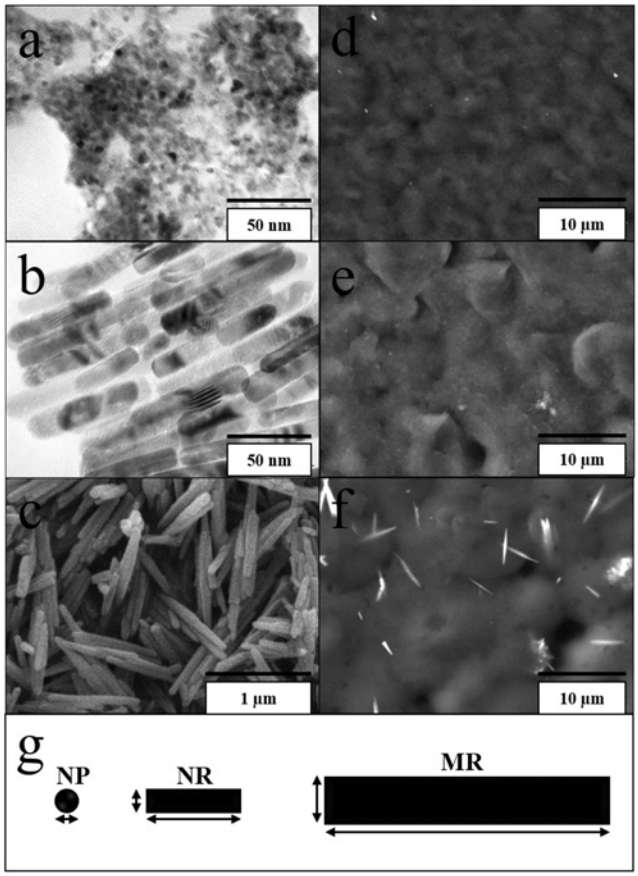

Fig. 2 *Morphology of synthesised ZnO*
a TEM image of ZnO NPs
b TEM image of ZnO NRs
c SEM image of MRs. The distribution of NPs in a polymer matrix was shown by means of backscattering mode of SEM;
d NPs,
e NRs,
f MRs
g Sketch depicted for each nanostructure

The percentage of crystallinity of semi-crystalline P(VDF-HFP) was given by (8) and the calculations for all cases were collected in Table 1

$$\%\text{crystallinity} = \frac{A(\text{peak})}{A(\text{total})} \times 100 \tag{8}$$

where A is an intensity at 2θ.

Fig. 4 shows the absorption spectra in the range of infrared, that corresponding to the mode of vibration of chemical bonding, via FT-IR. The absorption bands at 489, 614, 766, 795, 855, and 976 cm^{-1} indicated the α-phase of PVDF, while 840 cm^{-1} acted as a characteristic of the β-phase [18]. The addition of ZnO in P(VDF-HFP) decreased the absorption peak of the β-phase in MRs. The relative fraction of β-phase or the electroactivity has its maximum value at 2 wt% for both NPs and NRs inserted.

The material elasticity of the polymer-based composites is much better when compared with the bare polymer. The elastic modulus value is the best at 2 wt% for each particle type. However, the concentration >2 wt% may cause the agglomeration of the particles. This can be inherent internal defects that most pronounced in the case of NPs and resulted in a decrease in the elastic modulus. The highest elasticity occurred in the MRs type. This implies that the sample consisted of well-bonded particles so that the applied stress between particles and matrix effectively transferred.

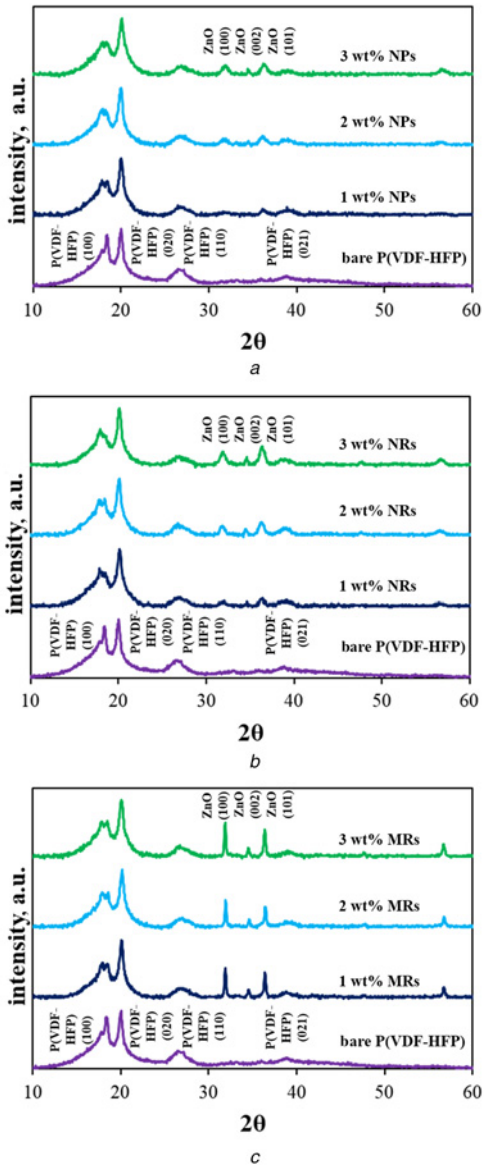

Fig. 3 *XRD patterns of the P(VDF-HFP) films with different concentrations and forms ZnO*
a NPs
b NRs
c MRs

Table 1 summarises the material properties for different amounts of NPs, NRs, and MRs ZnO. The polymer-based films with NRs and MRs have slightly higher crystalline phase and larger elastic modulus compared with NPs. The best value for the active phase derived from the addition of ZnO was found in 2 wt% NRs of ZnO.

3.3. Electro-mechanical properties: Plots of the dielectric constant of the samples measured at room temperature in a range of frequency between 1 and 20,000 Hz were shown in Fig. 5. The values increased with respect to the ZnO fractions and decrease with increments of the frequency. The phenomenon derived by nanoscale dimension has been described by Yamada *et al.* [23]. Spherical-like structure with high surface area possesses higher dielectric constant. This has been proved by the zeta potential (ZetaPALS, Brookhaven). A resulted potential of 25.78 ± 1.83 mV at the zeta layer of NPs indicated the existence of a lot of fixed charges at the prepared films. This implies that the NRs and NPs increase the capacitance of the polymer, leading to the enhancement of the dielectric constant of the films.

Table 1 Material properties of P(VDV-HFP) with various concentrations of ZnO of different shapes

P(VDF-HFP)		Crystallinity, %	Electro-activity	Elasticity, GPa
ZnO	Concentration, wt%			
—	0	46.21	0.34	1.89 ± 0.30
NPs	1	46.21	0.47	2.66 ± 0.60
	2	46.38	0.54	2.68 ± 0.67
	3	46.02	0.49	1.80 ± 0.25
NRs	1	46.09	0.49	3.24 ± 0.36
	2	46.26	0.51	3.36 ± 0.39
	3	46.23	0.49	2.57 ± 0.33
MRs	1	47.58	0.48	3.16 ± 0.32
	2	47.98	0.43	4.43 ± 0.70
	3	48.04	0.39	3.42 ± 0.41

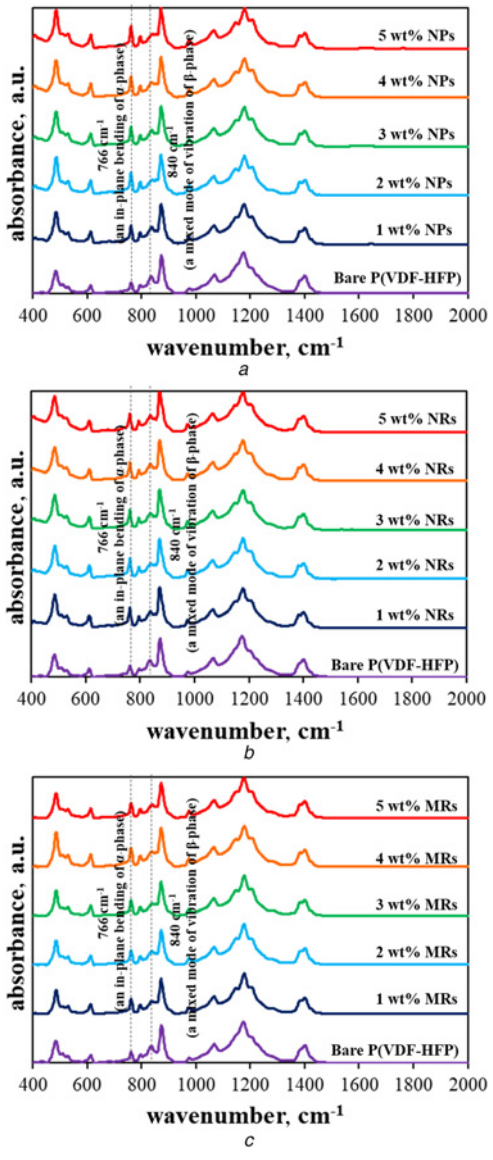

Fig. 4 *FT-IR spectrum of the P(VDF-HFP) films with different concentrations and forms ZnO*
a NPs
b NRs
c MRs

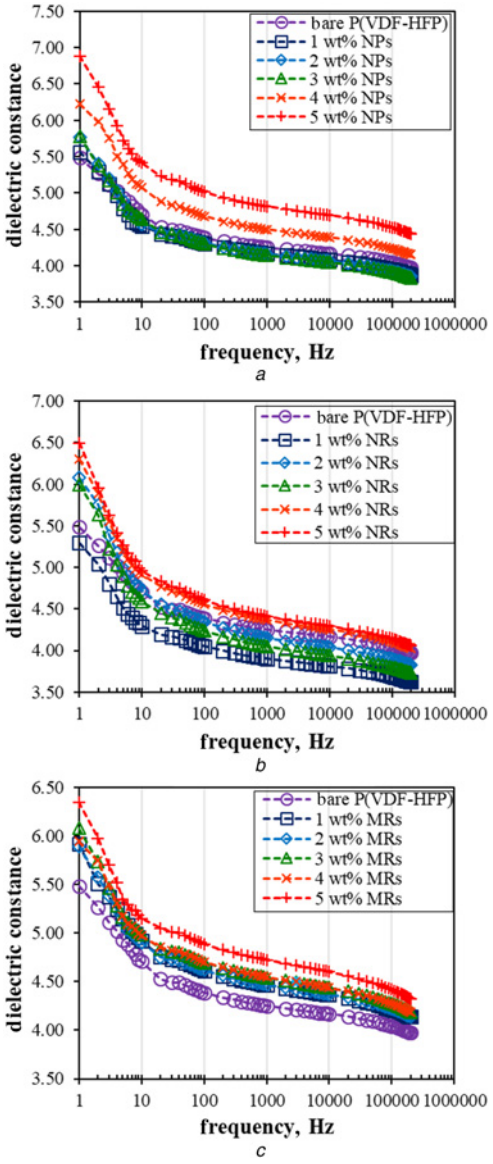

Fig. 5 *Plots of dielectric constant as functions of frequency for P (VDF-HFP)NPs with ZnO*
a NPs
b NRs
c MRs

The open-circuit voltage output of each sample was summarised in Fig. 6*a*. The optimum condition was 2, 3, and 4 wt% for NRs, MRs, and NPs, respectively. From the results, the 2 wt% NRs inserted sample is a choice for power harvesting test. From Fig. 6*b*, the AC power of the bare P(VDF-HFP) was only 0.35 µW while 2 wt% NRs in P(VDF-HFP) reached 1.12 µW.

doi: 10.1049/mnl.2018.0148

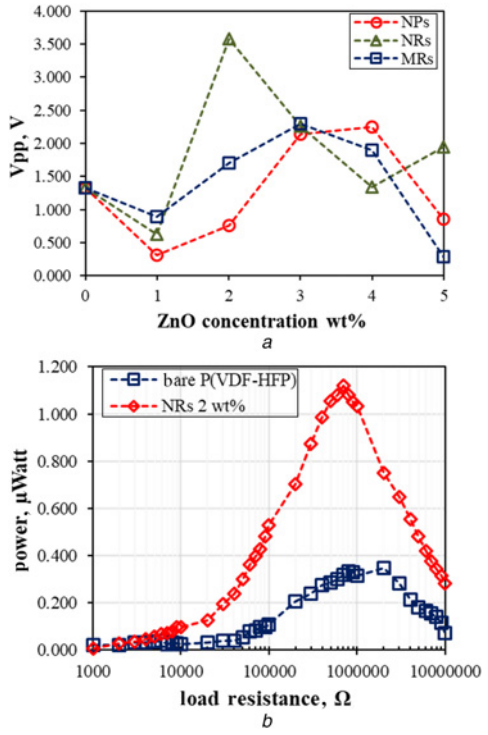

Fig. 6 *Curves of*
a Open-circuit voltage output with different concentrations and forms of ZnO
b Obtained power with respect to the load resistance compared between bare P(VDF-HFP) and P(VDF-HFP) with 2 wt% NRs ZnO

The optimum resistance was reduced accordingly from 2 MΩ to 700 kΩ. For a piezoelectric material under cyclically applied force, the figure-of-merit or the product of piezoelectric $(d_{31} \times g_{31})$ coefficients is perpendicular to generating power [8]. This means that the P(VDF-HFP) matrix inserted with 2 wt% NRs ZnO has developed the energy harvesting performance for a given configuration. As the cantilever was vibrated at 32 Hz, the polymer composite is able to harvest on low vibration level.

4. Conclusion: The P(VDF-HFP) has been incorporated with ZnO of different forms, i.e. NPs, NRs, and MRs. The polymer has been activated the piezoelectric phase with the poling filed of 70 MV/m at 90°C for 10 min. ZnO of various particle types is grown into piezoelectric wurtzite. The addition of ZnO has slightly changed the degree of crystallinity of the polymers and clearly increased the elasticity to the best value in the case of inserted MRs. The electroactive phase of the polymer-based film has been enhanced at 2 wt% of ZnO for both NPs and NRs cases. The dielectric constant of the films increased with ZnO concentration. Finally, a cantilever beam structure with the patch of P(VDF-HFP) reinforced with ZnO of 2 wt% NRs shows the best performance as a microsource of the energy of about 1 µW. Development of micropower energy harvesting in P(VDF-HFP) with ZnO NRs has been substantially and highly promising to power small-scale electronics.

5. Acknowledgments: The authors acknowledge the financial supports from the Royal Golden Jubilee Ph.D. Program under grant no. PHD/0034/2553, the Department of Physics, and the Graduate School, Prince of Songkla University, Hat Yai, Songkhla, Thailand. The authors thank Prof. Dr. Andrei Kholkin for sharing their knowledge on the AFM technique. Thanks to Ms. Sirirat Ouiganon for helping hands.

6 References

[1] Kawai H.: 'The piezoelectricity of poly(vinylidene fluoride)', *Japan J. Appl. Phys.*, 1969, **8**, pp. 975
[2] Ikeda T.: 'Fundamental of piezoelectricity' (Oxford Science Publications, New York, 1990)
[3] Das-Gupta D.K.: 'Ferroelectric polymers and ceramic-polymer composites' (Tran Tech Publ, Zurich, 1994)
[4] Whatmore R.W.: 'Pyroelectric ceramics and devices for thermal infra-red detection and imaging', *Ferroelectrics*, 1991, **118**, pp. 241–259
[5] Uchino K.: 'Ferroelectric devices' (Marcel Dekker, New York, 2000)
[6] Phermpornsakul Y., Muensit S., Guy I.L.: 'Determination of piezoelectric and pyroelectric coefficients and thermal diffusivity of 1–3 PZT/epoxy composites', *IEEE Trans. Dielect. Electr. Insul.*, 2004, **11**, (2), pp. 280–285
[7] Beeby S.P., Torah R.N., Tudor M.J.: 'A micro electromagnetic generator for vibration energy harvesting', *J. Micromech. Microeng.*, 2007, **17**, p. 1257
[8] Sukwisute P., Muensit N., Soontaranon S., *ET AL.*: 'Micropower energy harvesting using poly(vinylidene fluoride hexafluoropropylene)', *Appl. Phys. Lett.*, 2013, **103**, p. 063905
[9] Zhang L., Ding Y., Povey M., *ET AL.*: 'Zno nanofluids – a potential antibacterial agent', *Prog. Nat. Sci.*, 2008, **18**, (8), pp. 939–944
[10] Shalumon K.T., Anulekha K.H., Nair Sreeja V., *ET AL.*: 'Sodium alginate/poly(vinyl alcohol)/nano ZnO composite nanofibers for antibacterial wound dressings', *Int. J. Biol. Macromol.*, 2011, **49**, pp. 247–254
[11] Xu S., Qin Y., Xu C., *ET AL.*: 'Self-powered nanowire devices', *Nat. Nanotechnol.*, 2010, **5**, pp. 366–373
[12] Zhu G., Yang R., Wang S., *ET AL.*: 'Flexible high-output nanogenerator based on lateral ZnO nanowire array', *Nano Lett.*, 2010, **10**, pp. 3151–3155
[13] Hu Y., Lin L., Zhang Y., *ET AL.*: 'Replacing a battery by a nanogenerator with 20 V output', *Adv. Mater.*, 2012, **24**, pp. 110–114
[14] Parangusan H., Ponnamma D., Ali S.M., *ET AL.*: 'Stretchable electrospun PVDF-HFP/Co-ZnO nanofibers as piezoelectric nanogenerators', *Sci. Rep.*, 2018, **8**, p. 754
[15] Harnack O., Pacholski C., Weller H., *ET AL.*: 'Rectifying behavior of electrically aligned ZnO nanorods', *Nano Lett.*, 2013, **3**, pp. 1097–1101
[16] Greene L.E., Law M., Goldberger J., *ET AL.*: 'Low-temperature wafer-scale production of ZnO nanowire arrays', *Angew. Chem. Int. Ed.*, 2003, **42**, pp. 3031–3034
[17] Gregorio R., Cestari M.: 'Effect of crystallization temperature on the crystalline phase content and morphology of poly(vinylidene fluoride)', *J. Polym. Sci. B. Polym. Phys.*, 1994, **32**, pp. 859–870
[18] Martinsa P., Lopesa A.C., Lanceros-Mendeza S.: 'Electroactive phases of poly(vinylidene fluoride) determination, processing and applications', *Prog. Polym. Sci.*, 2014, **39**, pp. 683–706
[19] Hertz H.: 'On the contact of elastic solids', *J. Reine. Angew. Math.*, 1881, **92**, pp. 156–171
[20] Cappella B., Silbernagl D.: 'Nanomechanical properties of mechanical double-layer: a novel semiempirical analysis', *Langmuir*, 2007, **23**, pp. 10779–10787
[21] Jain A., Prashanth K.J., Sharma A., *ET AL.*: 'Dielectric and piezoelectric properties of PVDF/PZT composites: a review', *Polym. Eng. Sci.*, 2015, **55**, (7), pp. 1589–1616
[22] Özgür Ü., Alivov Y.I., Liu C., *ET AL.*: 'A comprehensive review of ZnO materials and devices', *J. Appl. Phys.*, 2005, **98**, p. 041301
[23] Yamada T., Ueda T., Kitayama T.: 'Piezoelectricity of a high-content lead zirconate titanate/polymer composite', *J. Appl. Phys.*, 1982, **53**, (6), p. 4328